Probability Distribution of Torsional Response by Q–Δ Resonance of Multi-Story Building under Long-Period Seismic Motion

Masayuki Kohiyama
Professor, Dept. of System Design Engineering, Keio University, Yokohama, Japan

ABSTRACT: When the torsional moment owing to geometric nonlinearity synchronizes with the torsional mode response, an internal resonance phenomenon occurs in a building structure system. The author's research group calls this phenomenon *Q–Δ* resonance. The probability distribution of the torsional response was evaluated using Monte Carlo simulations on a 60-story building model, the input wave being simulated using nonstationary colored-noise ground motion. The results showed that the torsional response greatly increased the horizontal acceleration response and the response amplification ratio between the center and corner of the top floor could exceed 1.2 when the model satisfied the *Q–Δ* resonance condition that the natural frequency of the torsional second mode matched the sum of the first natural frequencies in the *x*- and *y*-directions. It was also evident that closer proximity to the resonance condition increased the amplification ratio. These results suggest that *Q–Δ* resonance may need to be considered in seismic design.

1. INTRODUCTION

It has generally been believed that torsional response occurs in eccentric buildings with a poor balance between stiffness and mass (Anagnostopoulos *et al.* 2015). However, the author's research group has pointed out that even a biaxially symmetrical building could have a considerable torsional response due to internal resonance phenomena caused by geometric nonlinearity (Kohiyama *et al*. 2021). The principle can be explained as follows: consider a column with a biaxially symmetrical cross-section in which the top and bottom faces are horizontally constrained and which has different horizontal stiffness in the two directions. Let the *x*- and *y*-axis be the directions of higher and lower stiffness, respectively, and let k_x and k_y be the respective stiffnesses. If the top of the column is subjected to large displacements Δ_x and Δ_y in the *x*- and *y*-axis directions, restoring forces $Q_x = -k_x\Delta_x$ and $Q_y = -k_y\Delta_y$ are generated in the two directions, respectively. At this point, a torque of magnitude $(Q_x\Delta_y - Q_y\Delta_x)/2 = (k_x - k_y)\Delta_x\Delta_y/2$ must be applied to the upper and lower ends of the column to balance the moment of force around the member axis—that is, a large displacement of the column top generates a restoring torque.

The authors refer to this phenomenon as the *Q–Δ* effect. When the period of restoring torque generation coincides with the natural frequency of the torsional modes of the structural system, a large torsional response emerges due to the internal resonance phenomenon—the phenomenon being called *Q–Δ* resonance. The condition for the occurrence of *Q–Δ* resonance is when the sum or difference of the translational mode natural frequencies in the two horizontal directions coincides with the natural frequency of the torsional mode.

However, *Q–Δ* resonance does not occur unless large displacements occur in a building. Large magnitude earthquakes generate long-period seismic motions, which can reach distant locations without high attenuation. In the Great East Japan Earthquake, there was a case in which a super high-rise building 800 km away from the epicenter was seriously damaged. Since *Q–Δ* resonance is not considered at all in current seismic design, it may be a potential danger in high-rise buildings. Consequently, the aim of this study is to quantitatively understand the influence of *Q–Δ* resonance on high-rise buildings by conducting seismic response analysis considering geometric nonlinearity using simulated seismic motion.

2. METHODS: ANALYTICAL MODEL AND EQUATION OF MOTION

This study focuses on a shear-type building model. Material nonlinearities are not considered, with only geometric nonlinearities being taken into account. When the top and bottom faces of a column are horizontally constrained, the relationship between the forces acting on the bottom end 1 and top end 2 and the displacements of the two ends can be expressed by the following stiffness equations (Anamizu and Kohiyama 2023):

$$F_{x1} = -k_x(x_2 - x_1) - \frac{1}{2}(k_x - k_y)(y_2 - y_1)(\theta_1 + \theta_2) \quad (1)$$

$$F_{y1} = -k_y(y_2 - y_1) - \frac{1}{2}(k_x - k_y)(x_2 - x_1)(\theta_1 + \theta_2) \quad (2)$$

$$M_{z1} = -k_\theta(\theta_2 - \theta_1) + \frac{1}{2}(k_x - k_y)(x_2 - x_1)(y_2 - y_1) \quad (3)$$

$$F_{x2} = k_x(x_2 - x_1) + \frac{1}{2}(k_x - k_y)(y_2 - y_1)(\theta_1 + \theta_2) \quad (4)$$

$$F_{y2} = k_y(y_2 - y_1) + \frac{1}{2}(k_x - k_y)(x_2 - x_1)(\theta_1 + \theta_2) \quad (5)$$

$$M_{z2} = k_\theta(\theta_2 - \theta_1) + \frac{1}{2}(k_x - k_y)(x_2 - x_1)(y_2 - y_1) \quad (6)$$

where F_{xi}, F_{yi}, and M_{zi} (i = 1, 2) denote the x- and y-direction forces and the torsional torque around the z-axis (member axis) acting on column end i, respectively; x_i, y_i, and θ_i (i = 1, 2) denote the displacements in the x and y-directions and the rotation angle around the z-axis (counter-clockwise being positive) of end i, respectively; and k_x, k_y, and k_θ denote the shear stiffnesses in the x and y-directions and the torsional stiffness of the column, respectively. In these equations, the first terms correspond to linear restoring forces and the second nonlinear restoring forces owing to geometric nonlinearity.

Since the nonlinear restoring forces can be treated as external forces, the following equation of motion for a multi-story shear-type building model can be obtained:

$$\mathbf{M}\ddot{\mathbf{x}} + \mathbf{C}\dot{\mathbf{x}} + \mathbf{K}\mathbf{x} = -\mathbf{M}\ddot{\mathbf{x}}_0 + \mathbf{N}(\mathbf{x}) \quad (7)$$

where **M**, **C**, and **K** denote the stiffness, damping, and mass matrices, respectively; **x** and $\mathbf{x}_0$ denote the displacement vectors of the building model and ground, respectively; and **N**(**x**) denotes the external force vector owing to geometric nonlinearity.

The building model has 60 floors, the floor height being 4 m, and the floor plan dimensions being 50 × 30 m. The strong axis (x-axis) is in the long-side direction and the weak axis (y-axis) is in the short-side direction. The first natural period in the y-direction is 5 s (natural frequency f_{y1} = 0.2 Hz) and the first natural period in the x-direction is 4 s (natural frequency f_{x1} = 0.25 Hz). The mass of each layer is assumed to be 10^6 kg, and the moment of inertia can be obtained by assuming the radius of gyration to be 16.83 m. The stiffness of each story is set to achieve linear deformation when subjected to the seismic force specified in the Japanese building code. The torsional stiffness is assumed to be proportional to the stiffness in the translational direction, and is set so that the torsional second mode—that is, $f_{\theta 2} = f_{x1} + f_{y1}$ = 0.45 Hz (Model 1) or $f_{\theta 2} = f_{x1} + f_{y2}$ = 0.77 Hz (Model 2)—satisfies the Q–Δ resonance condition. Figure 1 shows the participation vectors for the first and second modes in each direction. With respect to the damping matrix **C**, a model of Wilson and Penzien (1972) is employed with a consistent damping factor of 1% for all modes. The simulated ground motions are input to the building model to evaluate the maximum response probability distribution.

The Ministry of Land, Infrastructure, Transport and Tourism of Japan has designated long-period design ground motion for high-rise buildings against possible large-scale earthquakes along the Nankai Trough (Building Research Institute, 2016). The target response spectrum for the Osaka area, OS1 (Figure 2) and an envelope function are used to generate colored-noise acceleration with nonstationary amplitude characteristics (Figure 3). Since a simulated ground motion is unidirectional, the motion is input at an angle of 45° with the northerly direction to provide bidirectional ground motion input in the *x*- and *y*-directions.

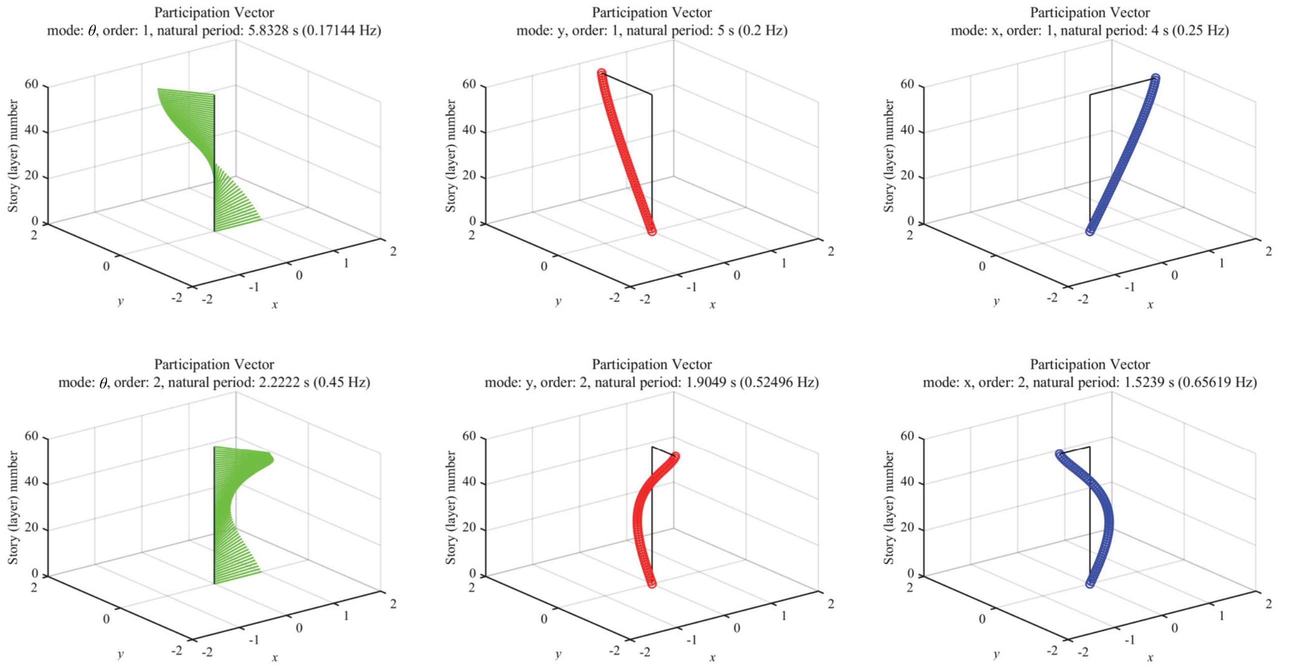

(a) Model 1 ($f_{\theta 2} = f_{x1} + f_{y1}$)

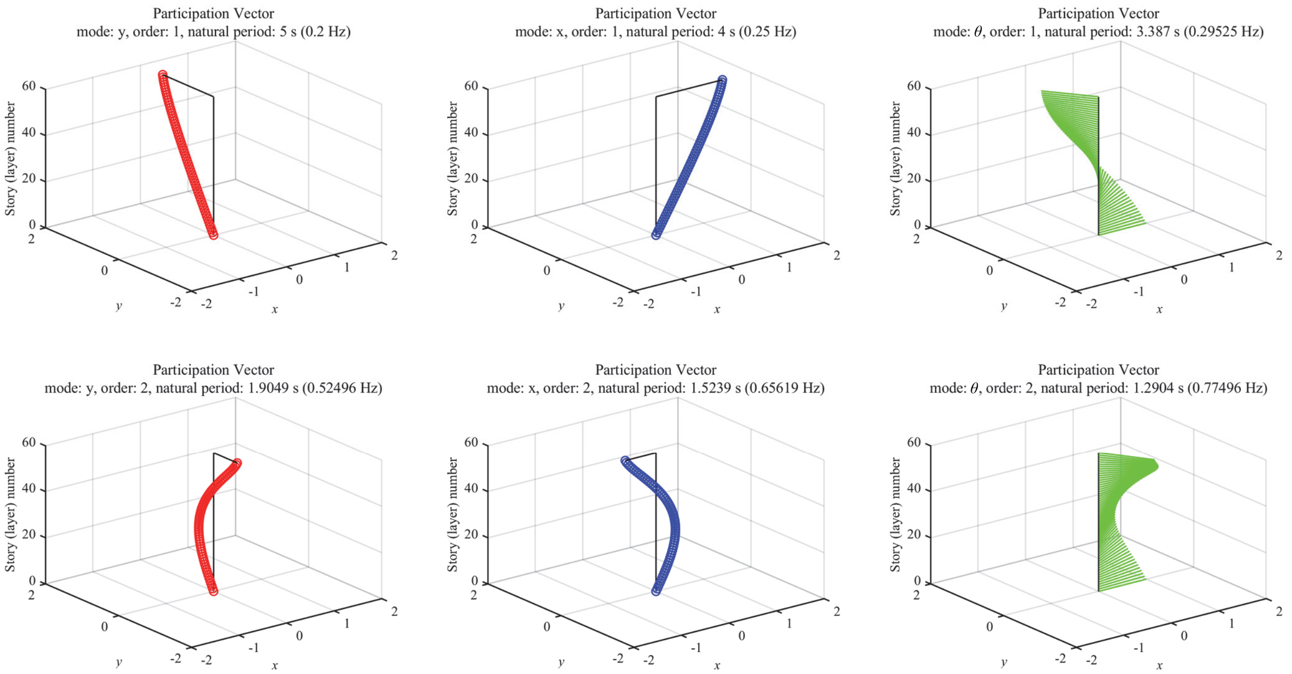

(b) Model 2 ($f_{\theta 2} = f_{x1} + f_{y2}$)

Figure 1: Participation vectors, natural periods, and natural frequencies of the two models.

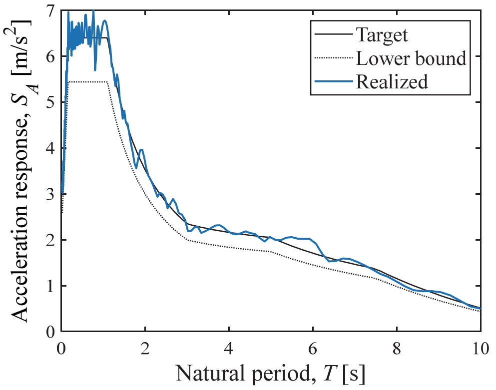

Figure 2: Target spectrum and acceleration response spectrum of realized ground motion example (damping factor of 5%).

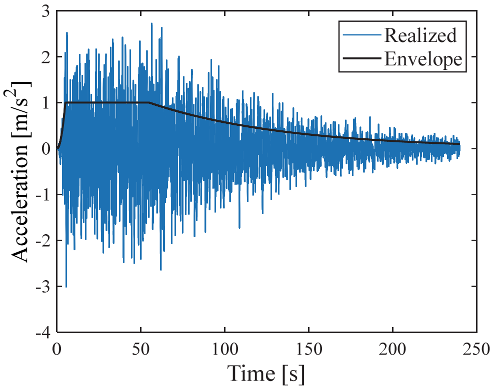

Figure 3: Example of realized ground motion.

3. ANALYTICAL RESULTS

Figure 4 and Figure 5 show the time histories of absolute acceleration and torsional displacement responses, respectively, at the top floor of two building models when the simulated ground motion shown in Figure 3 is input. It can be confirmed that Model 1 produces a relatively large torsional response (Figure 5(a)).

Although the deformation of the building model due to the torsional response is not at a level that would cause structural damage, the absolute acceleration response increases, especially at the corners of each floor. Consequently, focusing on the magnitude of the horizontal absolute acceleration response vector, we can analyses the maximum values at the corners (maximum values for both time and the four corners) against the maximum value at the center location for the top floor.

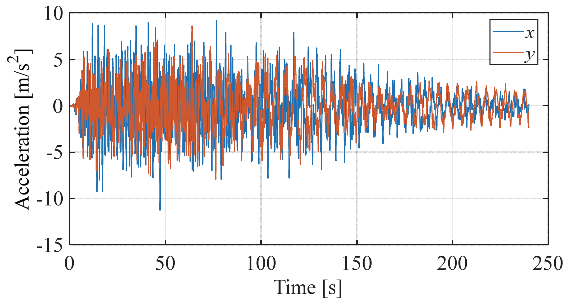

(a) Model 1 ($f_{\theta 2} = f_{x1} + f_{y1}$)

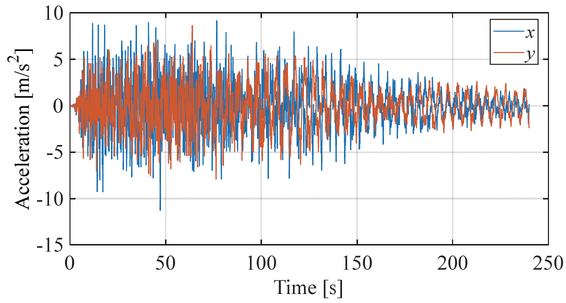

(b) Model 2 ($f_{\theta 2} = f_{x1} + f_{y2}$)

Figure 4: Time history of the top floor absolute acceleration response.

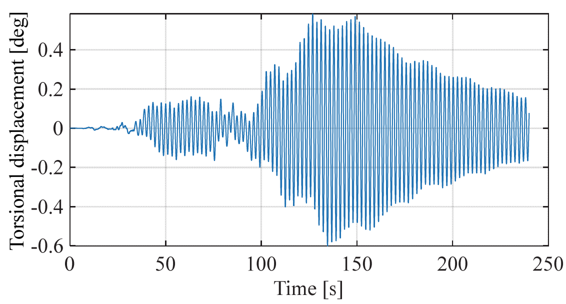

(a) Model 1 ($f_{\theta 2} = f_{x1} + f_{y1}$)

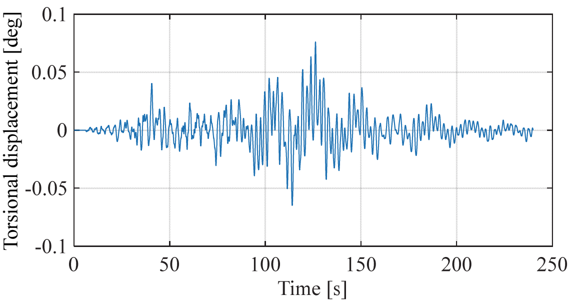

(b) Model 2 ($f_{\theta 2} = f_{x1} + f_{y2}$)

Figure 5: Time history of the top floor torsional displacement response.

To investigate the amplification ratio probability distribution of the maximum horizontal acceleration response, 1000 waves of simulated ground motion with different random phases were input to two models. Figure 6, Figure 7, and Figure 8 show the probability distributions of the maximum torsional displacement, the maximum horizontal acceleration at the center (A_{Cmax}) and corner (A_{Gmax}) of the top floor, and its amplification ratio, respectively. Again, it is evident that Model 1 tends to produce larger maximum responses than Model 2.

It should be noted that the amplification ratio of the maximum horizontal acceleration exceeds 1.2 in the case of Model 1 (Figure 8(a)), which is large, suggesting that the *Q–Δ* resonance phenomenon can cause an increase in response that structural engineers may not have anticipated. However, the probability is low and a more detailed analysis should be made of what the response would be if the *Q–Δ* resonance conditions are not perfectly satisfied.

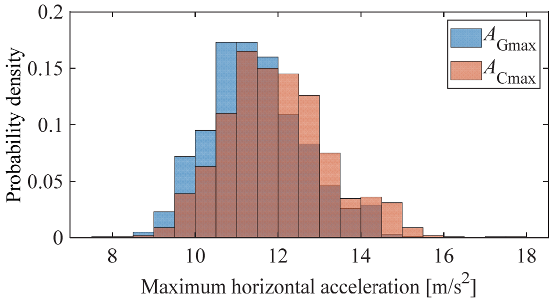

(a) Model 1 ($f_{\theta 2} = f_{x1} + f_{y1}$)

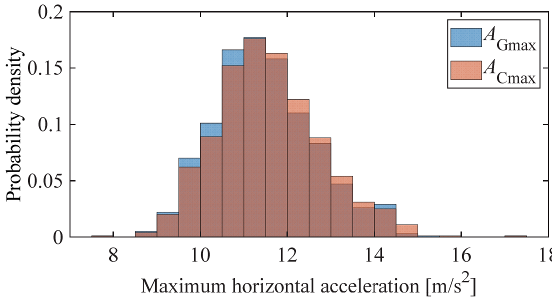

(b) Model 2 ($f_{\theta 2} = f_{x1} + f_{y2}$)

Figure 7: Probability distribution of the maximum horizontal acceleration at the center (A_{Gmax}) and the corner (A_{Cmax}) of the top floor.

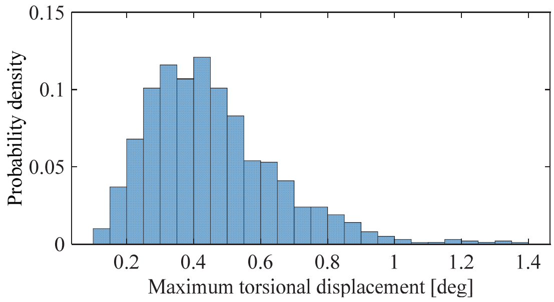

(a) Model 1 ($f_{\theta 2} = f_{x1} + f_{y1}$)

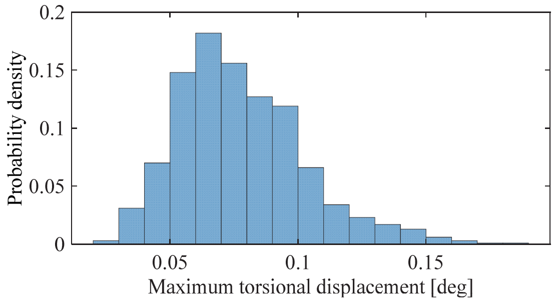

(b) Model 2 ($f_{\theta 2} = f_{x1} + f_{y2}$)

Figure 6: Probability distribution of the maximum torsional displacement of the top floor.

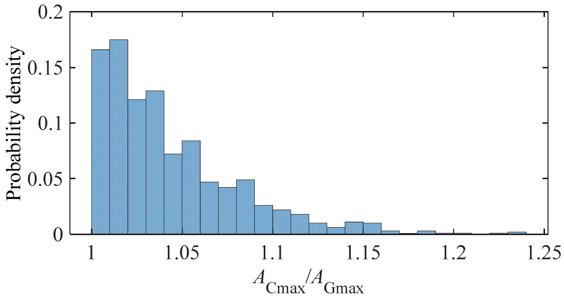

(a) Model 1 ($f_{\theta 2} = f_{x1} + f_{y1}$)

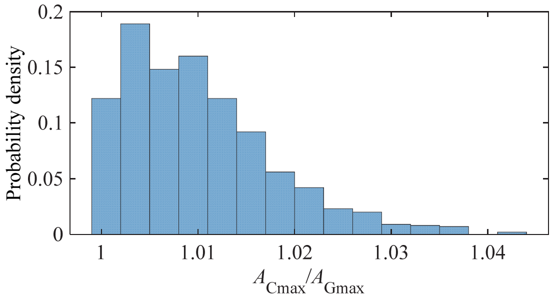

(b) Model 2 ($f_{\theta 2} = f_{x1} + f_{y2}$)

Figure 8: The amplification ratio probability distribution of the maximum horizontal acceleration between the corner and center of the top floor.

To examine the influence of the discordance in the *Q–Δ* resonance condition, the torsional stiffness of the models can be slightly modified. Figure 9 shows the amplification ratio probability distribution of the maximum horizontal acceleration, the horizontal axis representing the discordance of the *Q–Δ* resonance condition, δ:

$$\delta = \begin{cases} f_{\theta 2} / \left(f_{x1} + f_{y1} \right) & \text{(Model 1)} \\ f_{\theta 2} / \left(f_{x1} + f_{y2} \right) & \text{(Model 2)} \end{cases} \tag{8}$$

that is, the natural frequency of the second torsional mode to the frequency that matches the *Q–Δ* resonance condition.

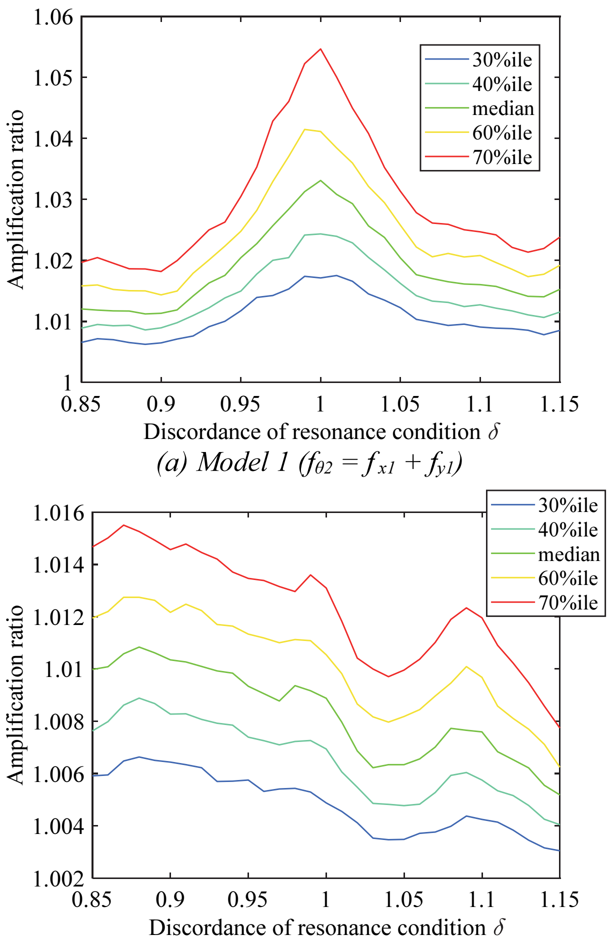

(a) Model 1 ($f_{\theta 2} = f_{x1} + f_{y1}$)

(b) Model 2 ($f_{\theta 2} = f_{x1} + f_{y2}$)

Figure 9: The amplification ratio probability distribution of the maximum horizontal acceleration.

In the case of Model 1, the percentile values of the acceleration amplification ratio at a top floor corner tend to increase with the proximity to the *Q–Δ* resonance condition. It is evident that the median value exceeds 1.03 when $\delta = 1$. In the case of Model 2, the response tends to increase, even on the low frequency side, possibly due to different resonance condition of other higher modes.

4. CONCLUSIONS

The effect of *Q–Δ* resonance was analyzed by inputting long-period, long-duration simulated ground motions to a 60-story shear-type building model. Consequently, it was evident that torsional response greatly increased the horizontal acceleration response, the response amplification ratio exceeding 1.2 when the model satisfied the *Q–Δ* resonance condition that the natural frequency of the torsional second mode matched the sum of the first natural frequencies in the *x*- and *y*-directions. At close proximity to the resonance condition, the percentile values of the horizontal acceleration of the top slab corner tended to increase with proximity to the resonance condition. These results suggest that *Q–Δ* resonance may need to be considered in seismic design.

However, the analysis does not consider material nonlinearity, which is an unrealistic assumption to make, especially in the *y*-direction where large displacements occur. When plastic deformation occurs, the stiffness is reduced and damping increases, resulting in a smaller torsional response.

Future work includes the same study for other *Q–Δ* resonance conditions, investigation using models with different parameters—such as building height and damping factor—examination of the response under different seismic motions, and analysis using a flexural-shear-type building model and considering material nonlinearity.

5. ACKNOWLEDGEMENTS

This work was financially supported by the SECOM Science and Technology Foundation and JSPS KAKENHI (Grant Number 20H02301).

6. REFERENCES

Anagnostopoulos, S. A., Kyrkos, M. T., and Stathopoulos, K. G. (2015). "Earthquake induced torsion in buildings: Critical review and state of the art", *Earthquakes and Structures*, 8(2), 305–377.

Anamizu, R. and Kohiyama, M. (2023). Study on a simplified model of a high-rise shear-type building for evaluation of Q–Δ resonance", *Journal of Structural and Construction Engineering (Transactions of AIJ)*, 88(803), 59–70.

Building Research Institute (2016). Special webpage for the release of technical information and data related to measures against long-period ground motion (in Japanese, title translated by the author), https://www.kenken.go.jp/japanese/contents/topics/lpe/index.html (last updated on 11 November 2021, accessed on 5 February 2023).

Kohiyama, M., Yokoyama, H., and Maki, S. (2022). "Torsional response of a bisymmetric structure induced by bending–torsion interaction in vertical members", *Japan Architectural Review*, 5(1), 3–19.

Wilson, E. L. and Penzien, J. (1972). "Evaluation of orthogonal damping matrices", *International Journal for Numerical Methods in Engineering*, 4(1), 5–10.